The FASEB Journal express article 10.1096/fj.03-1101fje**.** Published online April 14, 2004.

Angiogenesis in an in vivo model of adipose tissue development

Jaap G. Neels, Terri Thinnes, and David J. Loskutoff

The Scripps Research Institute, Department of Cell Biology, Division of Vascular Biology, La Jolla, California, USA.

Corresponding author: Prof. David J. Loskutoff, Ph.D., The Scripps Research Institute, Department of Cell Biology, Division of Vascular Biology, 10550 N. Torrey Pines Road, VB-3, La Jolla, CA 92037; E-mail: loskutof@scripps.edu

ABSTRACT

Obesity is associated with an increased risk for cardiovascular disease and cancer. Angiogenesis is a critical component of these pathological processes, and expanding adipose tissue represents one of the few sites of active angiogenesis in the adult. Despite the potential importance of angiogenesis in obesity, little is known about underlying mechanisms. This problem is magnified by the absence of useful quantitative model systems. In this report, we examine the angiogenic process using the 3T3-F442A model of adipose tissue development. In this model, 3T3-F442A preadipocytes are implanted subcutaneously into athymic Balb/c nude mice. We show that these cells develop into highly vascularized fat pads over the next 14–21 days, and that these fat pads are morphologically similar to normal subcutaneous adipose tissue. Histological studies demonstrate that a new microvasculature is evident as early as 5 days after cell implantation, and real-time quantitative RT-PCR analyses show that the expression of endothelial cell markers and adipogenesis markers increase in parallel during fat pad development. Finally, these preliminary studies suggest that the neovasculature originates by sprouting from larger, host-derived blood vessels that run parallel to peripheral nerves and that endothelial progenitor cells play little, if any, role in this process.

Key words: Obesity • neovascularization • adipocytes • endothelial cells • progenitor cells

Obesity has become a problem of epidemic proportions in Western societies, including the United States, and is commonly associated with a broad range of cardiovascular problems including accelerated atherosclerosis, increased risk for thrombosis, hypertension, hyperinsulinemia, insulin resistance, and type 2 diabetes (1). Excessive expansion of adipose tissue can result from adipocyte hypertrophy, a consequence of increased triglyceride storage, and/or from adipocyte hyperplasia, a process that requires the proliferation and differentiation of preadipocytes. Adipose tissue is highly vascularized, and increases in fat mass during the development of obesity in the adult appear to be accompanied by an increase in the size of the microcirculation (reviewed in (2, 3)). In this regard, there seems to be an absolute requirement for ongoing neovascularization during adipose tissue growth in mice since treatment of mice with angiogenesis inhibitors results in selective adipose tissue loss (4).

Although considerable information is available about the nature of factors that control adipocyte differentiation and metabolism, only limited information is available about the mechanisms of neovascularization during adipogenesis. Neovascularization and adipogenesis are spatially and temporally coupled during prenatal life, and paracrine interactions between endothelial cells (ECs) and adipocytes may mediate this coordinated growth (2, 3). In fact, adipocytes produce EC-specific mitogens and angiogenic factors (reviewed in (3)), while ECs produce soluble and matrix-bound mitogens that stimulate preadipocyte replication and differentiation (5–7). Adipose tissue is regularly used clinically to facilitate revascularization and healing of compromised or ischemic organs and tissues (8). Moreover, recent developments in reconstructive surgery have demonstrated the importance of the angiogenesis/adipogenesis relationship. For example, although autografting of fat pads has been the classical approach for the treatment of soft-tissue defects (9), progressive absorption of the graft with time has been a problem (10). Implantation of preadipocyte-seeded polymer scaffolds has been a promising improvement to this approach (11, 12). A recent study showed that subcutaneous injection of reconstituted basement membrane (Matrigel) in combination with the angiogenic basic fibroblast growth factor induces angiogenesis followed by adipose precursor cell recruitment and fat pad formation (13).

Although angiogenesis plays a critical role in the development of new blood vessels, it is now clear that other processes (e.g., endothelial progenitor cell (EPC) recruitment) may also contribute. Angiogenesis is characterized by the sprouting of ECs from preexisting blood vessels, and it relies on the proliferation, migration, and remodeling of these cells. EPCs circulate in the peripheral blood of adult mammals, including humans (reviewed in (14)) and can be recruited to target organs where they differentiate into mature ECs and are incorporated into the developing vessels (vasculogenesis) (14). The absence of suitable animal models has hindered attempts to delineate the relative importance of these and possibly other mechanisms of neovascularization during adipose tissue development.

In this report, we examine neovascularization during fat pad development using the 3T3-F442A model established by Green and Kehinde in 1979 (15). These investigators showed that 3T3-F442A cells underwent adipocyte conversion in culture, and developed into typical fat pads when injected subcutaneously into Balb/c (athymic) nude mice. More recently, the same model was employed to study leptin production in vivo (16). Although both studies focused on mechanisms of adipogenesis, both also demonstrated that the resulting fat pads were well supplied with blood vessels. We show that this model can be exploited to study mechanisms of neovascularization in the developing adipose tissue and can be conveniently used to monitor gene expression. These studies demonstrate that angiogenesis is the predominant mechanism of blood vessel formation in this model, and that the new vessels seem to sprout from nerve-associated blood vessels in the host. Importantly, EPCs play little, if any, role in the formation of this neovasculature.

METHODS

Animals and cell culture

Athymic BALB/c nude mice were maintained in a closed breeding colony at The Scripps Research Institute (TSRI). Tie2-GFP transgenic mice were from The Jackson Laboratory, Bar Harbor, ME. All experiments were performed in accordance with the NIH Guide for the Care and Use of Laboratory Animals, and all experimental procedures were approved by the TSRI

Animal Care and Use Committee. The 3T3-F442A cells were kindly provided by Dr. Howard Green (Harvard Medical School, Boston, MA) and cultured as described (17).

Production of fat pads in vivo

The in vivo model of adipogenesis was established essentially as described (15, 16). Briefly, 3T3-F442A preadipocytes (3×10^7 cells) were injected subcutaneously on the backs of 6- to 8-week-old athymic BALB/c nude mice. The cells grew and developed into mature lipid-laden fat pads over the next 3–4 weeks. At various times after implantation, mice were anesthetized with inhaled metofane, the fat pads were excised with the skin still attached, and the mice were killed by cervical dislocation. Normal inguinal fat was excised in parallel and employed as a control. Half of each fat pad and inguinal fat (stripped away from skin tissue) was cut into small pieces and either stored at –80°C for RNA isolation, or used for whole-mount-staining with fluorescent lectin as described below. The remaining half of each fat pad and inguinal fat (still attached to the skin) was fixed in Zn-formalin for 4 to 6 h, and then imbedded in paraffin for subsequent histological studies.

Histology and immunohistochemistry

Four-micrometer tissue sections were deparaffinized and then stained with hematoxylin and eosin (H&E) for histological analysis or were treated with methanol containing 0.3% H_2O_2 for 30 min for immunohistochemistry. Antigen retrieval and antibody staining were performed by standard procedures. The TSA Kit (Perkin-Elmer Life Sciences, Boston, MA) was employed for PECAM-1 and Green Fluorescent Protein (GFP) staining using either purified rat anti-mouse PECAM-1 monoclonal antibody (MEC 13.3; PharMingen, San Diego, CA) or rabbit anti-GFP (ab290; Novus Biolologicals, Littleton, CO). The bound antibodies were detected using biotin-conjugated rabbit anti-rat or goat anti-rabbit antiserum (Vector Laboratories, Burlingame, CA), with NovaRed (Vector Laboratories) used as the chromagen with hematoxylin counterstain. Rabbit anti-150 kD neurofilament (NF) polyclonal antibody (AB1981; Chemicon, Temecula, CA), and goat anti-rabbit biotin-conjugate were used to detect NF, and the ABC-Vectastain Elite ABC kit (Vector Laboratories) was used in combination with 3,3′-Diaminobenzidine (Zymed Laboratories, San Francisco, CA) for detection with hematoxylin counterstain. Sections stained as above but in the absence of the primary antibodies served as the negative controls.

Whole-mount lectin staining

Fat pad samples still attached to skin, were briefly (10–20 min) fixed in Zn-formalin, washed in 1× PBS containing 0.1 g/L $CaCl_2$, stripped from the skin, and cut into small (2 mm^3) tissue blocks. The tissue blocks were then incubated in the calcium-containing PBS in the dark for 48 h at 4°C in the presence of 10 μg/ml isolectin GS-IB_4 Alexa Flour 568 conjugate (Molecular Probes, Eugene, OR). After washing, the stained tissues were analyzed using a Biorad 1024 MRC scanning laser-confocal microscope. Z-serial images were merged using Lasersharp software (Biorad) to obtain a 3-D impression of the fat pad samples.

RNA isolation and quantitative real-time RT-PCR

Total RNA was isolated from frozen tissues and analyzed by quantitative real-time PCR as described previously (18), using the following gene-specific primer sets (Invitrogen):

β-actin-F (5′-TGGAATCCTGTGGCATCCATGAAAC-3′),
β-actin-R (5′-TAAAACGCAGCTCAGTAACAGTCCG-3′),
TIE1-F (5′-GCCCTTTTAGCCTTGGTGTG-3′),
TIE1-R (5′-CTTCACCCGATCCTGACTGG-3′),
TIE2-F (5′-CGGCCAGGTACATAGGAGGAA-3′),
TIE2-R (5′-CCCCCACTTCTGAGCTTCAC-3′),
FLT4-F (5′-CGAGACTGGAAGGAGGTGAC-3′),
FLT4-R (5′-GTACGTGTAGTTGTCCGCCC-3′),
PECAM1-F (5′-CTGGGAGGTCGTCCATGT-3′),
PECAM1-R (5′-CACAGGACTCTCGCAATCC-3′),
LpL-F (5′-TTCTCCTCCTACTCCTCCTC-3′),
LpL-R (5′-TGTCCTCAGCTGTGTCTTCA-3′),
adipsin-F (5′-TCCGCCCCTGAACCCTACAA-3′),
adipsin-R (5′-TAATGGTGACTACCCCGTCA-3′),
PAI-1-F (5′-TCAGAGCAACAAGTTCAACTACACTGAG-3′),
PAI-1-R (5′-CCCACTGTCAAGGCTCCATCACTTGCCCCA-3′),
TNFα-F (5′-GGCAGGTCTACTTTGGAGTCATTGC-3′),
TNF-α-R (5′-ACATTCGAGGCTCCAGTGAATTCGG-3′),
VEGFA-F (5′-TTACTGCTGTACCTCCACC-3′),
VEGFA-R (5′-ACAGGACGGCTTGAAGATG-3′).

We used total RNA from three different fat pads for each single time point and control inguinal fat, and all experiments were performed in duplicate. Quantification of a given gene, expressed as relative mRNA level compared with the sample with the lowest level of that specific mRNA, was calculated after normalization to β-actin RNA and using the $\Delta\Delta C_T$ formula as described by Perkin-Elmer. The specificity of the PCR amplification was verified by melt–curve analysis of the final products directly in the iCycler. Final data were represented in bar graphs with standard error bars using Sigma Plot software (RockWare, Golden, CO).

Bone marrow transplantations

Bone marrow cells were obtained by flushing the femurs and tibias from 8–10 week old Tie2-GFP donor mice with DMEM containing 5% FBS and 10 mM HEPES. The cells were washed twice by centrifugation, and then 2×10^6 viable cells (trypan blue staining) were administered via the tail vein to recipient athymic BALB/c nude mice 4–6 weeks of age. These mice were subjected to total body irradiation (1000 cGy; ^{137}Cs source) 3 h earlier. After allowing 4 weeks for the complete reconstitution of the bone marrow (monitored by PCR for GFP), the mice were injected subcutaneously with 3T3-F442A preadipocytes, and fat pad development was monitored as above.

Cell tracer studies

3T3-F442A preadipocytes were labeled fluorescent green by using the Vybrant CFDA SE Cell Tracer Kit according to the manufacturer's instructions (Molecular Probes, Eugene, OR). The

labeled cells were collected by centrifugation, mixed 1:1 with unlabeled cells, and injected subcutaneously into athymic BALB/c nude mice. Fat pad development was monitored as above.

Results

Morphology of developing fat pads

Figure 1 shows the morphology of the fat pads at different times. The injected cells were retained within a pocket formed by the fascia, a layer of connective tissue that separates the skin from the underlying muscle tissue, and thus did not spread from the site of injection. Within 24 h, this pocket of cells could be dissected from the mouse as a semisolid structure (not shown), and the fat pads which developed from it at later times were easily identified (Fig. 1*A*), and could be surgically removed (Fig. 1*B* and *C*). Microscopic examination revealed that the central core of the fat pad rapidly became necrotic (Fig. 1*D*), possibly because of an inadequate blood supply to this region. However, the outer layer of cells survived and began to differentiate into mature adipocytes. At three weeks, this layer of cells had expanded in size and developed into a highly vascularized fat pad (Fig. 1*E*) that morphologically resembled control subcutaneous adipose tissue. By this time, the necrotic core had largely disappeared, leaving a stretch of scar tissue in the middle (Fig. 1*E*, arrowheads).

Kinetics of neovascularization during fat pad development

To define the kinetics of neovascularization during fat pad development, paraffin sections from fat pads harvested at different times were stained for PECAM-1, a marker for ECs (Fig. 2*A–F*). New microvessels were evident as early as 5 days (Fig. 2*B*), and some of these contained red blood cells (not shown) and thus appeared to be functional. PECAM-1 positive neovasculature was detected by day 10 throughout the developing fat pad (Fig. 2*C*) and by day 21 (Fig. 2*E*), their morphology began to resemble that of the control subcutaneous adipose tissue (inguinal fat; Fig. 2*F*). Similar results were obtained when the neovasculature was visualized by whole-mount laser confocal microscopy using an EC specific fluorescent-labeled lectin (Fig. 2*G–L*).

Analysis of gene expression during fat pad development

Fat pads encapsulated by the fascia were relatively easy to separate from the attached skin (Fig. 1), enabling us to employ quantitative real-time RT-PCR to monitor changes in the expression of EC and adipogenesis marker genes as a function of time (Fig. 3*A–F*). As expected, none of the EC markers (i.e., TIE-1, TIE-2, FLT-4, and PECAM-1) were expressed by the injected preadipocytes (not shown), and relatively little expression was detected during the first day of fat pad development (Fig. 3*A–D*). However, significant expression of each gene was apparent by day 3, reaching a plateau by day 6. The increase in these mRNAs reflects the increasing number of ECs in the developing fat pads, with subsequent neovascularization. By three weeks, most of the EC marker genes were expressed at similar levels as those in control subcutaneous adipose tissue. The expression of two adipogenesis marker genes, lipoprotein lipase (LpL) (Fig. 3E) and adipsin (Fig. 3F), like that of the EC marker genes, was marginal early during fat pad development, steadily increased with time, and by 3 weeks, was similar to that observed in control subcutaneous adipose tissue. We also analyzed the gene expression profile of plasminogen activator inhibitor-1 (PAI-1), tumor necrosis factor α (TNFα), and vascular endothelial growth factor A (VEGFA), three angiogenic factors known to be expressed in

adipose tissue (Fig. 3*G–I*) (19–21). Although PAI-1 mRNA was barely detectable in the preadipocytes before injection (not shown), the levels were very high at day 1 of fat pad development, decreasing thereafter (Fig. 3*G*). Besides demonstrating angiogenic activity (22), TNFα was previously shown to induce PAI-1 in adipose tissue (23). Again, TNFα mRNA was barely detected in the preadipocytes before injection (data not shown), but was transiently up-regulated early in fat pad development (Fig. 3*H*). VEGFA mRNA levels also transiently increased during the first days of fat pad development (Fig. 3*I*). The dramatic but transient induction of PAI-1, and to a lesser extent TNFα and VEGFA, raises the possibility that these genes may contribute to subsequent angiogenesis events. This possibility is currently under investigation.

Origin of the neovasculature in developing fat pads

Experiments were performed to investigate the origin of the ECs that form the new vasculature in the expanding adipose tissue. Three possibilities were considered, including recruitment of EPCs, conversion of the 3T3-F442A cells into ECs, and sprouting from existing host vessels.

Role of EPCs

In recent years, bone marrow-derived EPCs were shown to participate in normal and pathological postnatal neovascularization (reviewed in (14)). To investigate the potential contribution of EPCs to the observed neovascularization, fat pads were grown in athymic nude mice that had previously received a bone marrow transplantation from transgenic TIE2-GFP donor mice (Fig. 4). Because these transgenic mice constitutively express GFP under the transcriptional regulation of the EC-specific TIE2 promotor (24), GFP expression should be restricted to ECs in the vasculature. The resulting fat pads were harvested at various times and then were stained either with PECAM-1 to visualize the vasculature, or with GFP to determine the degree of EPC incorporation into it. An immunological approach, instead of GFP fluorescence, was used to detect GFP-positive cells because the fluorescent signal was lost as a result of tissue processing. Initial control experiments demonstrated that subcutaneous (i.e., inguinal) adipose tissue from the parental transgenic TIE2-GFP mouse gave a similar pattern for both PECAM-1 staining (Fig. 4*A*) and GFP staining (Fig. 4*B*). Thus, the staining protocol detects GFP under the conditions employed, and GFP is specifically expressed in ECs. Although a PECAM-1 positive neovasculature was observed in the developing fat pads from day 5 on (Fig. 4*C*; see also Fig. 2*B–E*), no GFP positive ECs were detected in any of the sections (Fig. 4*D*), except those occasionally observed in the 14-day old fat pads (Fig. 4*E*). In this regard, a total of 10 fat pads were harvested (i.e., 2 fat pads each on days 1, 5, 11, 14, and 21) and at least 2 sections per fat pad were stained for GFP. Of the 20 sections examined, only sections from the 14-day-old fat pad were positive, showing a few GFP-stained ECs in some vessel walls (compare Fig. 4*D* with Fig. 4*E*). The very low number of GFP-positive ECs detected in these experiments suggests that these cells play little if any role in the neovascularization of the developing fat pads.

Role of the injected 3T3-F442A cells

It is known that 3T3-L1 cells can express an EC phenotype under some conditions (25). The 3T3-F442A cell line employed here originated from the same parent cell line, thus raising the possibility that the neovasculature in the developing fat pads could be derived from the injected

cells themselves. To investigate this possibility, 3T3-F442A cells were labeled with a fluorescent green cell tracer stain, mixed with unlabeled cells, and then injected into the mice. The resulting fat pads were harvested at various times, stained with the fluorescent EC-specific lectin, and then analyzed by whole-mount laser confocal microscopy (Fig. 5). If the neovasculature was derived from the injected cells, then it should contain areas positive for both the lectin (red) and cell tracer (green). Figure 5*A* shows the border of a 1-week-old fat pad. At this early time, the lectin-stained vasculature appears to be invading into a mix of labeled (green) and unlabeled injected 3T3-F442A cells. The invading neovasculature lacks detectable 3T3-F442A cells (green). The center of this fat pad (Fig. 5*B*) lacked a defined vasculature. It consisted primarily of the mix of labeled and unlabeled cells, together with an occasional lectin-positive cell. By 10 days, the center of the fat pad (Fig. 5*C*) contained a well-defined lectin-positive vascular network together with individual green labeled cells. However, there were still no areas in which the vasculature was positive for both the cell tracer and lectin, and this was also true for 2-, 3-, and 4-week-old fat pads (not shown). Thus, the vasculature appears to be derived from the host and not from the injected cells.

Role of sprouting from pre-existing host vessels

Experiments were performed to determine whether angiogenesis (i.e., sprouting from preexisting blood vessels) is the mechanism of neovascularization in this model. Examination of a large number of fat pads by PECAM-1 staining revealed that although the fascia surrounding the fat pads varied in thickness, it remained largely devoid of vasculature at all times (see Fig. 1*D*, 2*C* and *D*, and 6*B* and *C*). Thus, the capillaries in the fat pads probably sprout from larger vessels that protrude through the fascia at select points. This appears to be the case since systematic analysis revealed the presence of vessels that protrude through the fascia at a limited number of specific areas (arrows Fig. 6*D–F*), and then sprout into capillaries in the fat pads. These protruding vessels seem to branch from other large blood vessels located outside the fascia. These vessels run parallel to nerve bundles (Fig. 6*D–F*). In fact, NF staining shows that the fat pad is surrounded by nerve bundles (arrowheads Fig. 6*A*) and that these nerve bundles are consistently associated with large blood vessels (representative example shown in Fig. 6*G*). These blood vessel-associated nerve bundles reside just outside the fascia (Fig. 6*A*) and are likely to be part of the sensory nervous system of the overlaying skin. These results suggest that the neovasculature in the developing fat pads is derived by sprouting from nerve-associated blood vessels.

DISCUSSION

Although angiogenesis is required for adipose tissue expansion in obesity (4), little is known about mechanisms that regulate the growth and remodeling of the vasculature in this condition. In this report we begin to address this issue using the 3T3-F422A in vivo model of adipose tissue development. Although this model was initially employed to study adipogenesis (15), we show that it also can be employed to study angiogenesis. Thus, a functional neovasculature was evident as early as 5 days after cell implantation, it continued to remodel and mature for the next 10–14 days, and by 21 days, it was morphologically (Fig. 2) and synthetically (Fig. 3) similar to the vasculature present in control subcutaneous adipose tissue. Importantly, the kinetics of neovascularization and adipogenesis seems to be reproducible as indicated by the relatively small standard errors observed for the expression of different genes (Fig. 3). Besides this reproducibility, the model was convenient for immunohistochemistry and gene profiling

experiments, and as indicated below, could be employed to study different aspects of fat pad development.

Link between angiogenesis and adipogenesis

Using this model, we demonstrated that there was a close spatial relationship between blood vessel development and adipogenesis. For example, immunohistochemical staining for PECAM-1 (Fig. 2*A–F*) demonstrated that the kinetics of angiogenesis in the fat pads paralleled the increase in the formation of lipid-filled vacuoles in the cells (Fig. 2*A–F*), a change that is characteristic of adipogenesis. In addition, gene expression profiling (Fig. 3) revealed an increase in the expression of EC marker genes that paralleled the increase in expression of adipogenic marker genes. In spite of the similar kinetics, these studies do not allow us to conclude that vascular development precedes adipogenesis in this model, or vice versa. The problem is that in some instances, mature lipid-laden adipocytes were detected in the absence of an apparent vasculature (not shown), raising the possibility that adipogenesis precedes angiogenesis. However, in other instances, some highly vascularized areas of fat pads seemed to contain considerably more mature adipocytes (not shown), suggesting that vascularization may promote adipogenesis. As discussed below, this inconsistency may reflect local differences in the composition and/or density of the extracellular matrix.

Factors that may influence vascular remodeling during fat pad development

Extensive crosstalk between adipocytes and ECs has been demonstrated (3, 5–7), and this bidirectional signaling seems to be mediated both by extracellular matrix components and by direct cell–cell interactions. It is likely that such crosstalk plays a role in coordinating angiogenesis and adipogenesis in the expanding adipose tissue. It is also clear that the anatomical location of the fat depot (i.e., subcutaneous vs. internal fat pads) may influence the extent and pattern of the vasculature (26) and may determine whether vascular development precedes or follows adipose tissue growth. Finally, there appears to be a link between the density of the connective tissue/collagen fibers and the rate of capillary and adipocyte maturation (2, 26). In this regard, a comparison of fetal perirenal and subcutaneous adipose tissues indicates that the formation of capillaries and the subsequent size of adipocyte clusters are inversely correlated with the degree of extracellular matrix deposition (2). Moreover, when 3T3-F442A preadipocytes were injected subcutaneously into nude mice, the presence of Matrigel decreased the rate of adipocyte and microvessel maturation (27). These observations suggest that the presence of a dense connective tissue may suppress adipogenesis by physically impairing the development of capillaries (2). Our observation that the fascia surrounding the developing fat pads was relatively devoid of vasculature (Fig. 6) supports this idea since the fascia is a layer of connective tissue which contains a dense collagen matrix.

Besides the composition and density of the extracellular matrix, hypoxia may also be an important driving force for vascular remodeling in expanding adipose tissue (3). Hypoxia is a potent inducer of angiogenesis, and the rapid development of the necrotic core (Fig. 1*D*) suggests a potential role for hypoxia in our model. The thickness of the outer layer of surviving preadipocytes denoted “developing fat pad” in Fig. 1*B* seems to be rather consistent (≈200μm), suggesting that this thickness defines the oxygen diffusion limit in this particular tissue. Although the development of regions of hypoxia remains to be demonstrated during the growth of adipose tissue in obesity, it is well known that adipocytes do respond to hypoxic stimulus by

increasing the production of leptin and other molecules (3). Moreover, the synthesis and secretion of hypoxia-inducible angiogenic factors are markedly increased in obesity (28–30). In this respect, it is of interest to note that the hypoxia-regulated angiogenic factors PAI-1 (31), TNFα (32), and VEGFA (33) were increased during the first days of fat pad development, coinciding with the development of the necrotic core. Whether the induction of those genes is important for subsequent angiogenic events remains to be determined. In any case, it is tempting to speculate that the expansion of adipose tissue is associated with local hypoxia and that this condition is, at least in part, responsible for the increased expression of angiogenic factors.

Properties of the neovasculature

The unique characteristics of specific vascular beds again depend on their anatomical location. Our observation that FLT-4 expression increases in parallel to that of PECAM-1, TIE-1, and TIE-2 was somewhat surprising, since this receptor was originally thought to be a specific marker for lymphatic endothelia (34), and adipose tissue has been described to lack lymphatics (35). However, FLT-4 was shown to be expressed in many fenestrated endothelia (36), and the adipose tissue was recently shown to contain fenestrated endothelia (37). On the basis of these findings, the increase in FLT-4 raises the possibility that neovascularization of the developing fat pads involves fenestrated endothelia. Fenestrated endothelium is usually present in capillaries of tissues where extensive molecular exchange occurs across the blood vessel wall (e.g., in endocrine glands and the kidney). This function would seem to be important for the adipose tissue because it actively releases leptin and a variety of regulatory molecules into the circulatory system (28, 30).

Origin of the vasculature

It has recently become apparent that circulating bone marrow-derived EPCs are involved in promoting physiologic and pathologic neovascularization during wound healing and tumor growth (14). Although the presence of EPCs in the circulation and within ischemic tissues has been clearly established, questions still remain regarding the magnitude of their contribution to newly forming blood vessels. In our model, EPCs were very rarely detected in the fat pad neovasculature (Fig. 4), suggesting that they do not play a major role in the formation of new vessels in this model. This conclusion is consistent with the recent observation that bone marrow-derived EPCs do not contribute to vascular growth and remodeling in a model of regenerative lung growth and alveolization in adult mice (38). However, EPCs clearly contribute to neovascularization in other models (39), possibly reflecting the use of angiogenic growth factors (39). Other differences that may alter the recruitment and participation of circulating EPCs include variation in mechanical or biophysical properties inherent to a specific vascular locus, the absence or presence of inflammatory stimuli, and the unique microenvironment within different organ beds.

The new vessels that develop in the 3T3-F422A-induced fat pads seem to originate predominantly by sprouting from larger blood vessels that run parallel to peripheral nerves. In peripheral tissues, nerves and blood vessels frequently enjoy a close anatomical relationship (40), one that is emphasized by the common branching patterns of nerves and blood vessels. It was recently shown that arteries, but not veins, are aligned with peripheral nerves, and that peripheral nerves seem to govern the pattern of blood vessel branching and arterial differentiation in the skin by the secretion of VEGF from sensory fibers and/or Schwann cells (41). These

observations raise the possibility that nerves could guide the patterning of the blood vessels in the fat pads as well. This possibility seems unlikely since the neovasculature was observed as early as 5 days after cell implantation, but the innervation of the fat pads was not evident until 6 weeks (not shown).

In summary, we have demonstrated that the 3T3-F442A in vivo fat pad model is well suited to study neovascularization of developing adipose tissue. In this preliminary report, we successfully employed this model in gene profiling experiments and to study the origin of the neovasculature. This model also should be useful to investigate the role of the extracellular matrix, fenestrated endothelia, hypoxia, and a variety of other factors on this process.

ACKNOWLEDGMENTS

This work was supported in part by NIH grant HL59549 (to D.J.L.). J.G.N. was supported by a Postdoctoral Fellowship Award from the American Heart Association. This is TSRI manuscript no. 16086-CB.

Note Added in Proof

After completion and submission of this paper for publication, the authors discovered a recent report by Fukumura et al. (42), which employed related approaches to shed new light on the complex interplay between adipogenesis and angiogenesis. This report shows that inhibition of adipocyte differentiation by transfection of preadipocytes with a peroxisome proliferator-activated receptor gamma dominant-negative construct not only abrogated fat tissue formation but also reduced angiogenesis. Moreover, inhibition of angiogenesis by a blocking antibody developed against vascular endothelial growth factor receptor-2 (VEGFR2), reduced angiogenesis and tissue growth, and also inhibited preadipocyte differentiation.

REFERENCES

1. Mokdad, A. H., Ford, E. S., Bowman, B. A., Dietz, W. H., Vinicor, F., Bales, V. S., and Marks, J. S. (2003) Prevalence of obesity, diabetes, and obesity-related health risk factors, 2001. *J. Am. Med. Assoc.* **289,** 76–79

2. Crandall, D. L., Hausman, G. J., and Kral, J. G. (1997) A review of the microcirculation of adipose tissue: Anatomic, metabolic, and angiogenic perspectives. *Microcirculation.* **4,** 211–232

3. Bouloumie, A., Lolmede, K., Sengenes, C., Galitzky, J., and Lafontan, M. (2002) Angiogenesis in adipose tissue. *Ann. Endocrinol.* **63,** 91–95

4. Rupnick, M. A., Panigrahy, D., Zhang, C. Y., Dallabrida, S. M., Lowell, B. B., Langer, R., and Folkman, M. J. (2002) Adipose tissue mass can be regulated through the vasculature. *Proc. Natl. Acad. Sci. U.S.A.* **99,** 10,730–10,735

5. Varzaneh, F. E., Shillabeer, G., Wong, K. L., and Lau, D. C. (1994) Extracellular matrix components secreted by microvascular endothelial cells stimulate preadipocyte differentiation in vitro. *Metabolism* **43,** 906–912

6. Hutley, L. J., Herington, A. C., Shurety, W., Cheung, C., Vesey, D. A., Cameron, D. P., and Prins, J. B. (2001) Human adipose tissue endothelial cells promote preadipocyte proliferation. *Am. J. Physiol. Endocrinol. Metab.* **281,** E1037–E1044

7. Aoki, S., Toda, S., Sakemi, T., and Sugihara, H. (2003) Coculture of endothelial cells and mature adipocytes actively promotes immature preadipocyte development in vitro. *Cell Struct. Funct.* **28,** 55–60

8. Silverman, K. J., Lund, D. P., Zetter, B. R., Lainey, L. L., Shahood, J. A., Freiman, D. G., Folkman, J., and Barger, A. C. (1988) Angiogenic activity of adipose tissue. *Biochem. Biophys. Res. Commun.* **153,** 347–352

9. Billings E., Jr., and May, J. W., Jr. (1989) Historical review and present status of free fat graft autotransplantation in plastic and reconstructive surgery. *Plast. Reconstr. Surg.* **83,** 368–381

10. Ersek, R. A. (1991) Transplantation of purified autologous fat: A 3-year follow-up is disappointing. *Plast. Reconstr. Surg.* **87,** 219–227

11. Patrick, C. W., Jr., Chauvin, P. B., Hobley, J., and Reece, G. P. (1999) Preadipocyte-seeded PLGA scaffolds for adipose tissue engineering. *Tissue Eng.* **5,** 139–151

12. Kral, J. G., and Crandall, D. L. (1999) Development of a human adipocyte synthetic polymer scaffold. *Plast. Reconstr. Surg.* **104,** 1732–1738

13. Toriyama, K., Kawaguchi, N., Kitoh, J., Tajima, R., Inou, K., Kitagawa, Y., and Torii, S. (2002) Endogenous adipocyte precursor cells for regenerative soft-tissue engineering. *Tissue Eng.* **8,** 157–165

14. Masuda, H., and Asahara, T. (2003) Post-natal endothelial progenitor cells for neovascularization in tissue regeneration. *Cardiovasc. Res.* **58,** 390–398

15. Green, H., and Kehinde, O. (1979) Formation of normally differentiated subcutaneous fat pads by an established preadipose cell-line. *J. Cell. Physiol.* **101,** 169–171

16. Mandrup, S., Loftus, T. M., MacDougald, O. A., Kuhajda, F. P., and Lane, M. D. (1997) Obese gene expression at in vivo levels by fat pads derived from sc implanted 3T3–F442A preadipocytes. *Proc. Natl. Acad. Sci. U.S.A.* **94,** 4300–4305

17. Green, H. and Kehinde, O. (1976) Spontaneous heritable changes leading to increased adipose conversion in 3T3-cells. *Cell* **7,** 105–113

18. Sartipy, P., and Loskutoff, D. J. (2003) Monocyte chemoattractant protein 1 in obesity and insulin resistance. *Proc. Natl. Acad. Sci. U.S.A.* **100,** 7265–7270

19. Samad, F., Yamamoto, K., and Loskutoff, D. J. (1996) Distribution and regulation of plasminogen activator inhibitor-1 in murine adipose tissue in vivo. Induction by tumor necrosis factor-alpha and lipopolysaccharide. *J. Clin. Invest.* **97,** 37–46

20. Hotamisligil, G. S., Shargill, N. S., and Spiegelman, B. M. (1993) Adipose expression of tumor necrosis factor-alpha: Direct role in obesity-linked insulin resistance. *Science* **259,** 87–91

21. Asano, A., Morimatsu, M., Nikami, H., Yoshida, T., and Saito, M. (1997) Adrenergic activation of vascular endothelial growth factor mRNA expression in rat brown adipose tissue: implication in cold-induced angiogenesis. *Biochem. J.* **328,** 179–183

22. Frater-Schroder, M., Risau, W., Hallmann, R., Gautschi, P., and Bohlen, P. (1987) Tumor necrosis factor type alpha, a potent inhibitor of endothelial cell growth in vitro, is angiogenic in vivo. *Proc. Natl. Acad. Sci. U.S.A.* **84,** 5277–5281

23. Samad, F., Uysal, K. T., Wiesbrock, S. M., Pandey, M., Hotamisligil, G. S., and Loskutoff, D. J. (1999) Tumor necrosis factor alpha is a key component in the obesity-linked elevation of plasminogen activator inhibitor 1. *Proc. Natl. Acad. Sci. U.S.A.* **96,** 6902–6907

24. Motoike, T., Loughna, S., Perens, E., Roman, B. L., Liao, W., Chau, T. C., Richardson, C. D., Kawate, T., Kuno, J., Weinstein, B. M., Stainier, D. Y. R., and Sato, T. N. (2000) Universal GFP reporter for the study of vascular development. *Genesis* **28,** 75–81

25. Zangani, D., Darcy, K. M., Masso-Welch, P. A., Bellamy, E. S., Desole, M. S., and Ip, M. M. (1999) Multiple differentiation pathways of rat mammary stromal cells in vitro: acquisition of a fibroblast, adipocyte or endothelial phenotype is dependent on hormonal and extracellular matrix stimulation. *Differentiation* **64,** 91–101

26. Hausman, G. J., Wright, J. T., and Thomas, G. B. (1991) Vascular and cellular development in fetal adipose tissue: Lectin-binding studies and immunocytochemistry for laminin and Type-IV collagen. *Microvasc. Res.* **41,** 111–125

27. Kawaguchi, N., Toriyama, K., Nicodemou-Lena, E., Inou, K., Torii, S., and Kitagawa, Y. (1999) Reconstituted basement membrane potentiates in vivo adipogenesis of 3T3-F442A cells. *Cytotechnology* **31,** 215–220

28. Caro, J. F., Sinha, M. K., Kolaczynski, J. W., Zhang, P. L., and Considine, R. V. (1996) Leptin: The tale of an obesity gene. *Diabetes* **45,** 1455–1462

29. Straczkowski, M., Dzienis-Straczkowska, S., Stepien, A., Kowalska, I., Szelachowska, M., and Kinalska, I. (2002) Plasma interleukin-8 concentrations are increased in obese subjects and related to fat mass and tumor necrosis factor-alpha system. *J. Clin. Endocrinol. Metab.* **87,** 4602–4606

30. Loskutoff, D. J. and Samad, F. (1998) The adipocyte and hemostatic balance in obesity: studies of PAI-1. *Arterioscler. Thromb. Vasc. Biol.* **18,** 1–6

31. Fitzpatrick, T. E. and Graham, C. H. (1998) Stimulation of plasminogen activator inhibitor-1 expression in immortalized human trophoblast cells cultured under low levels of oxygen. *Exp. Cell Res.* **245,** 155–162

32. Scannell, G., Waxman, K., Kaml, G. J., Ioli, G., Gatanaga, T., Yamamoto, R., and Granger, G. A. (1993) Hypoxia induces a human macrophage cell line to release tumor necrosis factor-alpha and its soluble receptors in vitro. *J. Surg. Res.* **54,** 281–285

33. Shweiki, D., Itin, A., Soffer, D., and Keshet, E. (1992) Vascular endothelial growth factor induced by hypoxia may mediate hypoxia-initiated angiogenesis. *Nature* **359,** 843–845

34. Kaipainen, A., Korhonen, J., Mustonen, T., Vanhinsbergh, V. W. M., Fang, G. H., Dumont, D., Breitman, M., and Alitalo, K. (1995) Expression of the Fms-Like Tyrosine Kinase-4 Gene Becomes Restricted to Lymphatic Endothelium During Development. *Proc. Natl. Acad. Sci. U.S.A.* **92,** 3566–3570

35. Ryan, T. J. (1995) Lymphatics and adipose tissue. *Clin. Dermatol.* **13,** 493–498

36. Partanen, T. A., Arola, J., Saaristo, A., Jussila, L., Ora, A., Miettinen, M., Stacker, S. A., Achen, M. G., and Alitalo, K. (2000) VEGF-C and VEGF-D expression in neuroendocrine cells and their receptor, VEGFR-3, in fenestrated blood vessels in human tissues. *FASEB J.* **14,** 2087–2096

37. Cao, R., Brakenhielm, E., Wahlestedt, C., Thyberg, J., and Cao, Y. (2001) Leptin induces vascular permeability and synergistically stimulates angiogenesis with FGF-2 and VEGF. *Proc. Natl. Acad. Sci. U.S.A.* **98,** 6390–6395

38. Voswinckel, R., Ziegelhoeffer, T., Heil, M., Kostin, S., Breier, G., Mehling, T., Haberberger, R., Clauss, M., Gaumann, A., Schaper, W., and Seeger, W. (2003) Circulating vascular progenitor cells do not contribute to compensatory lung growth. *Circ. Res.* **93,** 372–379

39. Murayama, T., Tepper, O. M., Silver, M., Ma, H., Losordo, D. W., Isner, J. M., Asahara, T., and Kalka, C. (2002) Determination of bone marrow-derived endothelial progenitor cell significance in angiogenic growth factor-induced neovascularization in vivo. *Exp. Hematol.* **30,** 967–972

40. Burnstock, G. and Ralevic, V. (1994) New insights into the local-regulation of blood flow by perivascular nerves and endothelium. *Br. J. Plast. Surg.* **47,** 527–543

41. Mukouyama, Y., Shin, D., Britsch, S., Taniguchi, M., and Anderson, D. J. (2002) Sensory nerves determine the pattern of arterial differentiation and blood vessel branching in the skin. *Cell* **109,** 693–705

42. Fukumura, D., Ushiyama, A., Duda, D. G., Xu, L., Tam, J., Krishna, V., Chatterjee, K., Garkavtsev, I., and Jain, R. K. (2003) Paracrine regulation of angiogenesis and adipocyte differentiation during in vivo adipogenesis. *Circ. Res.* **93,** e88–e97

Received December 18, 2003; accepted March 9, 2004.

Fig. 1

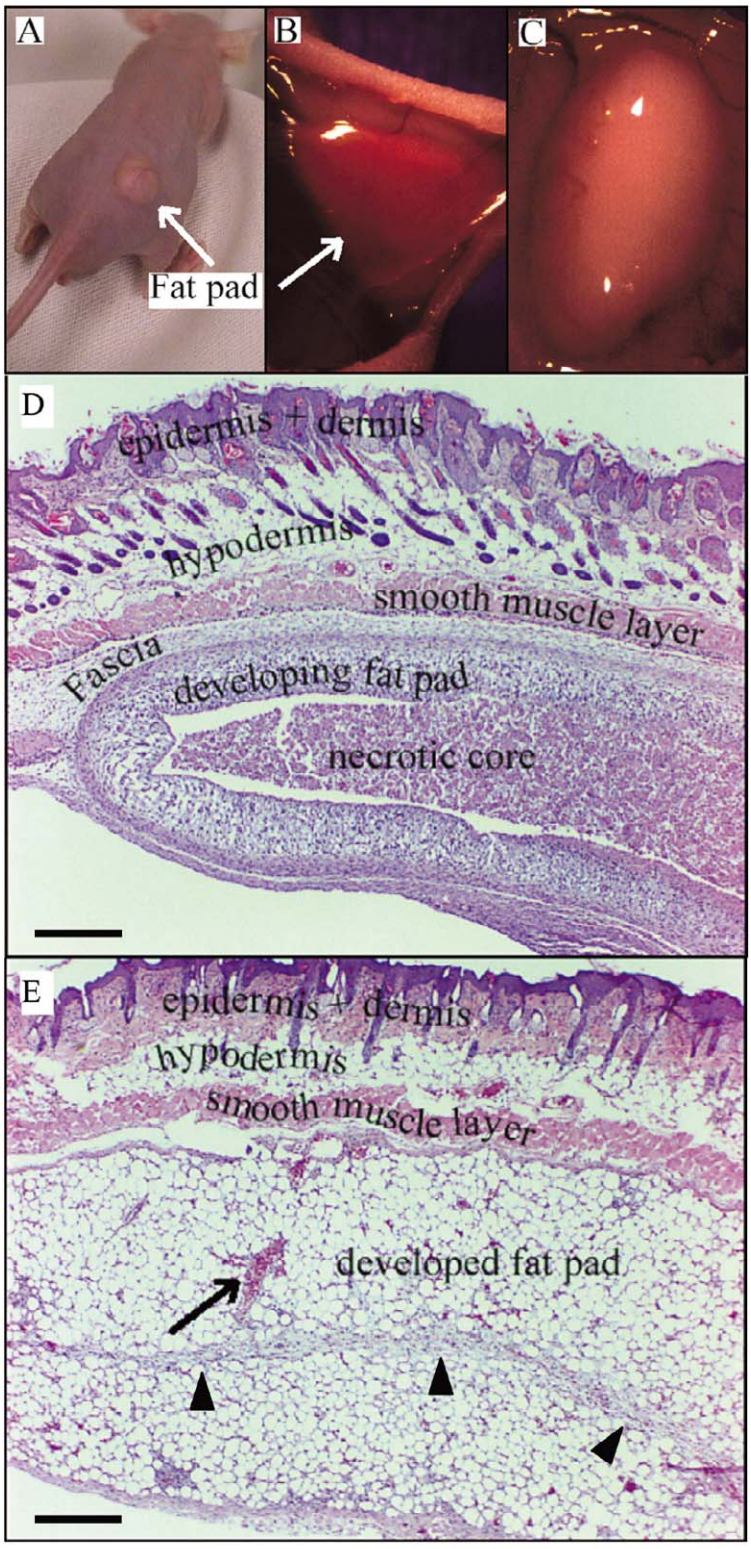

Figure 1. Morphology of developing fat pads. Photographs of a 1-week old developing fat pad (***A***) clearly visible on the back of a mouse, of a 10-day old fat pad (***B***) with the skin peeled back to reveal the fascia (the shiny membrane) that encapsulates it, and of a 3-day old fat pad (***C***) removed from the mouse but still attached to the skin. H&E-stained sections from a 4-day old fat pad (***D***) with the different layers of the skin and fat pad indicated, and from a 21-day old fat pad (***E***) showing the scar that remains from where the necrotic core was resorbed (arrowheads). The arrow indicates a relatively large blood vessel present in the fat pad. Scale bar in (***D*** and ***E***) = 250 μm.

Fig. 2

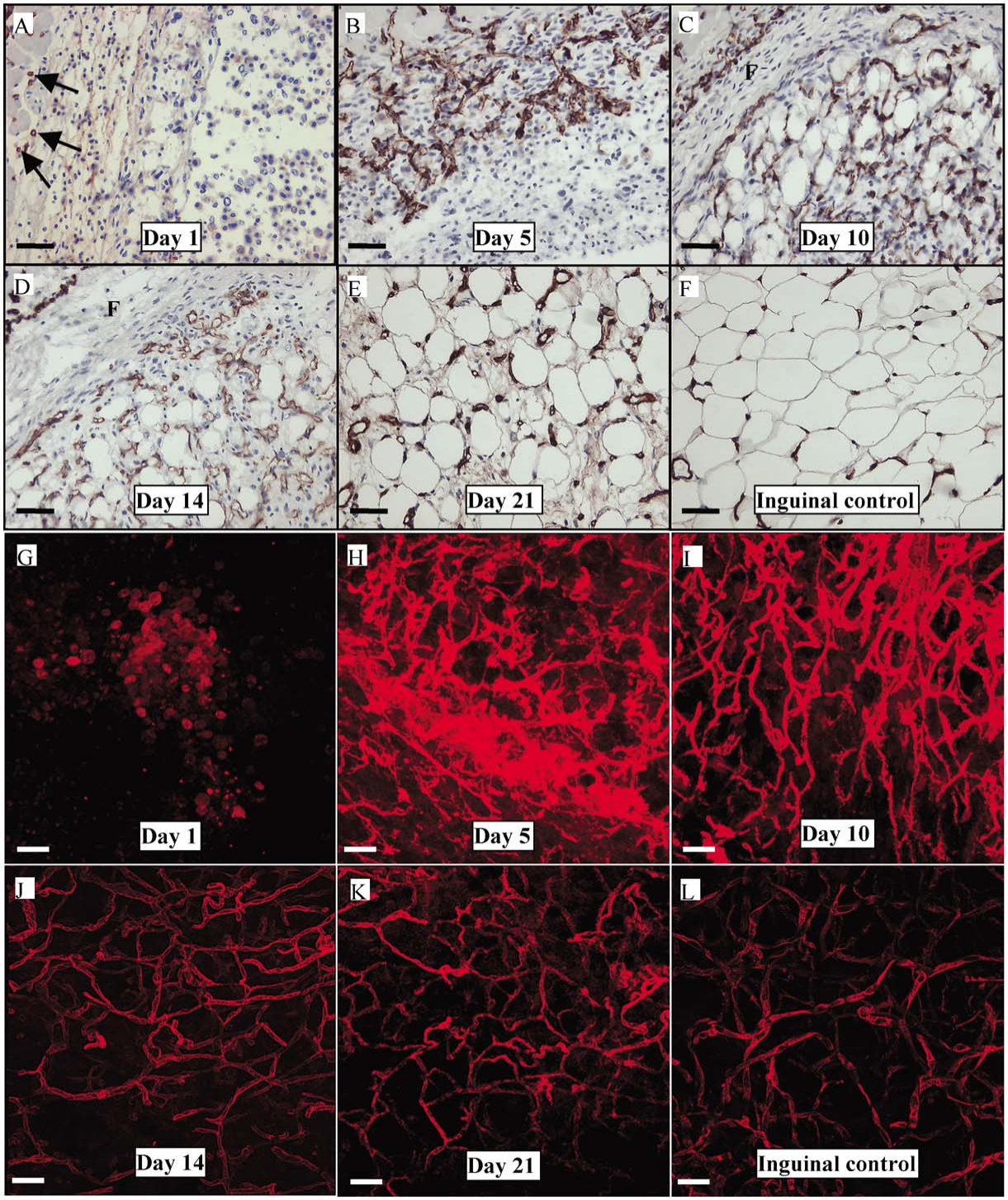

Figure 2. Kinetics of neovascularization during fat pad development. Sections of fat pads harvested at the indicated different times and stained to reveal blood vessels. (***A–F***) Immunohistochemical staining for the EC marker PECAM-1 (brown color). Arrows at day 1 (***A***) indicate capillaries observed in the muscle layer of the skin (left border of photograph) but not in the injected layer of preadipocytes (right half of photograph). The letter F indicates the fascia. (***G–L***) 3D-imaging results of whole mounts of tissue samples stained with fluorescent IB_4 lectin and then were analyzed by laser-confocal microscopy. Sections (Z-series) were merged and the resulting images are shown. Scale bar = 50 μm.

Fig. 3

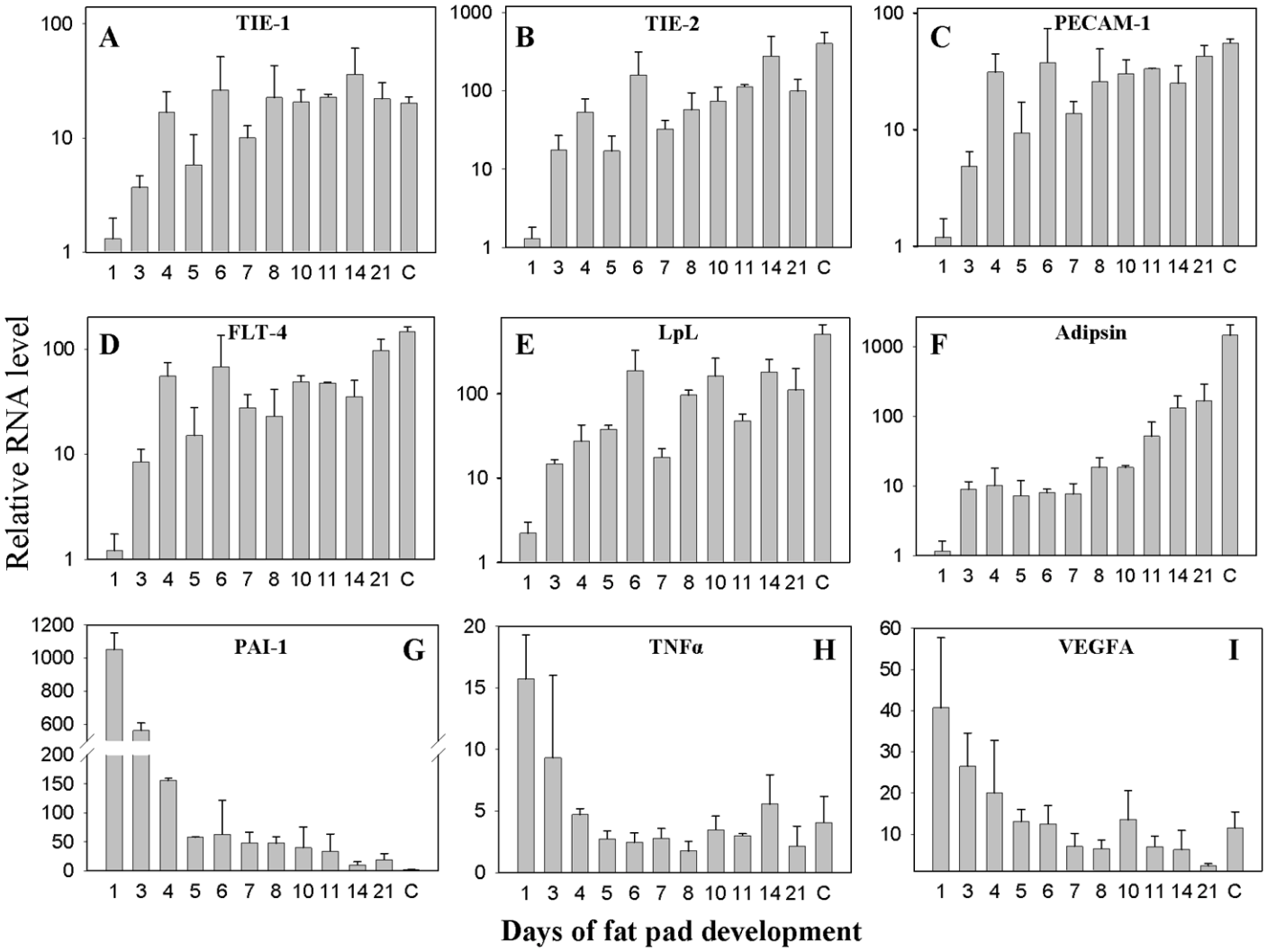

Figure 3. Quantitative real-time RT-PCR analysis of gene expression during fat pad development. Total RNA was prepared from developing fat pads at the indicated times and then was analyzed for the expression of EC marker genes (***A–D***), adipogenesis (***E, F***) marker genes, and angiogenic factors (***G–I***) by quantitative real-time RT-PCR. (***A***) TIE-1; (***B***) TIE-2; (***C***) PECAM-1; (***D***) FLT-4; (***E***), lipoprotein lipase; (***F***) adipsin; (***G***) PAI-1; (***H***) TNFα; (***I***) VEGFA. Error bars represent standard errors ($n = 3$).

Fig. 4

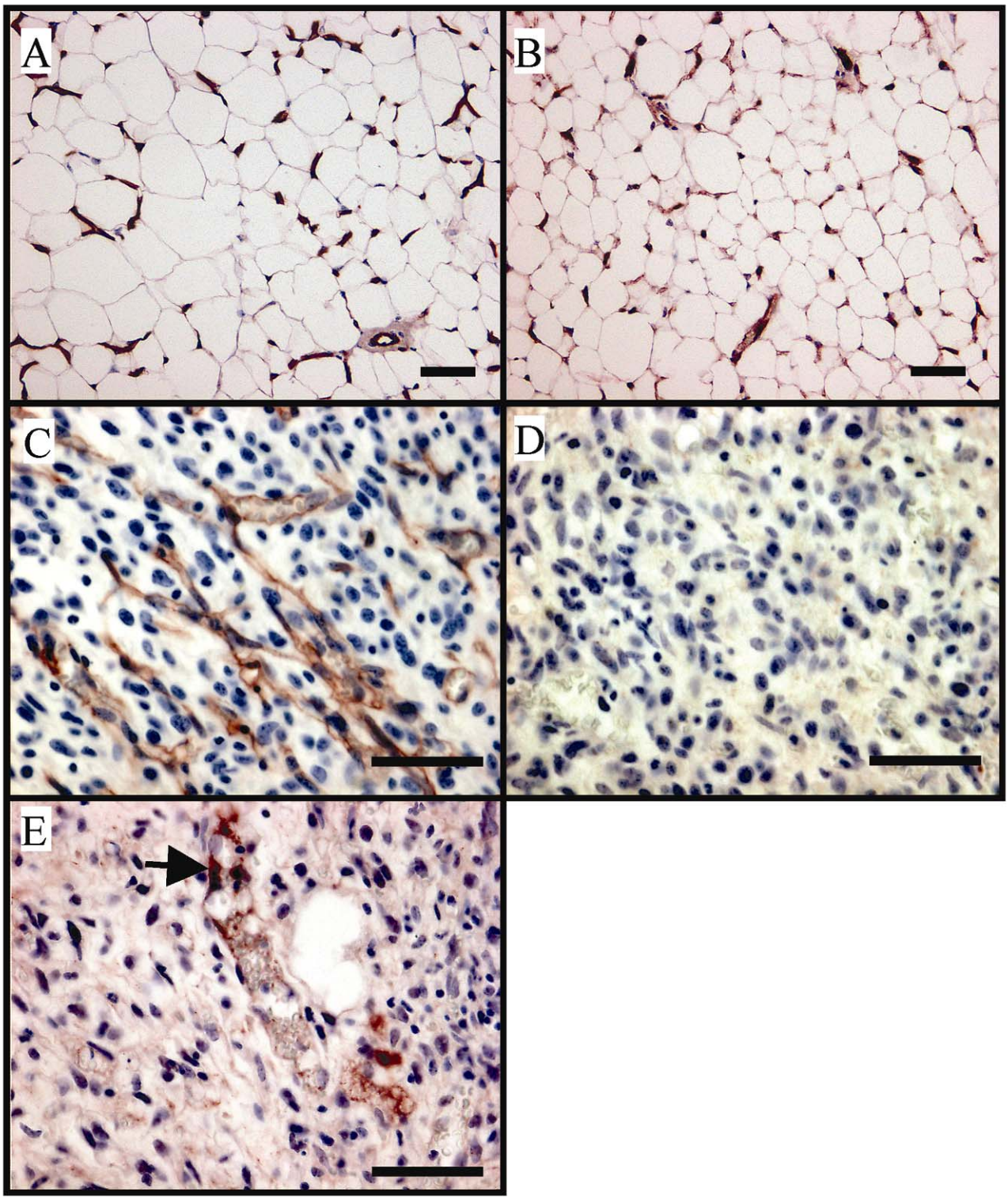

Figure 4. Behavior of EPCs in developing fat pads. Immunohistochemical staining (brown color) for PECAM-1 (***A***, ***C***) and GFP (***B***, ***D***, and ***E***). (***A***, ***B***) staining patterns of inguinal adipose tissue derived from a Tie2-GFP transgenic mouse. (***C–E***) staining patterns of (***C, D***) 11-day and a (***E***) 14-day old fat pad grown in athymic nude mice that had previously received bone marrow from a Tie2-GFP transgenic mouse. Arrow indicates the presence of GFP positive EPCs as part of the neovasculature. Scale bar = 50 μm.

Fig. 5

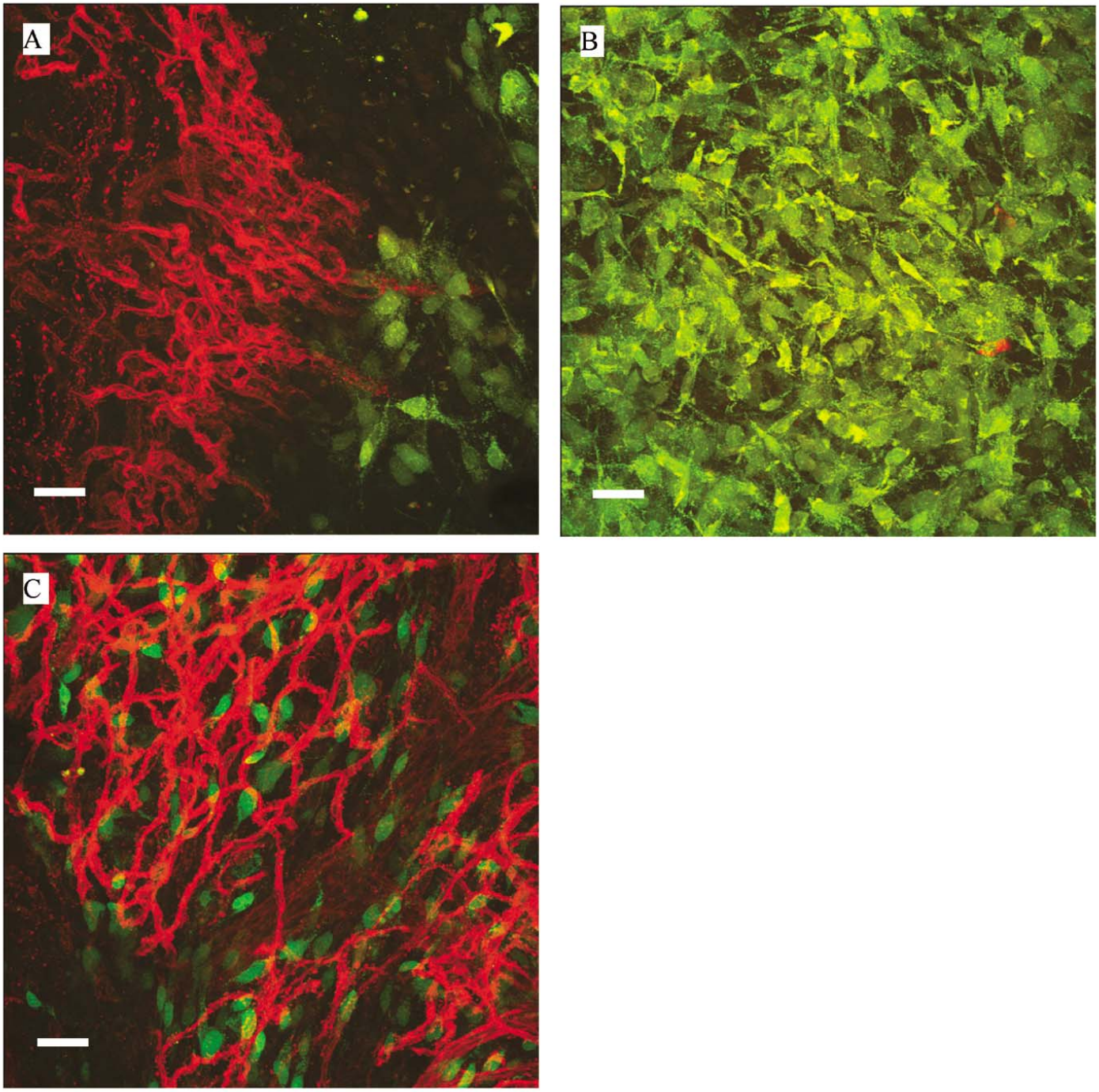

Figure 5. Behavior of injected 3T3-F442A cells in developing fat pads. Laser confocal images of whole mounts of fat pads which develop after injection of a 1:1 mix of 3×10^7 fluorescently labeled (green) with unlabeled 3T3-F442A cells. The tissues were then stained with EC-specific fluorescent lectin (red). (***A***) shows the border of a 1-week-old fat pad, (***B***) shows the center of the same fat pad, and (***C***) shows the center of a 10-day-old fat pad. Scale bar = 50 μm.

Fig. 6

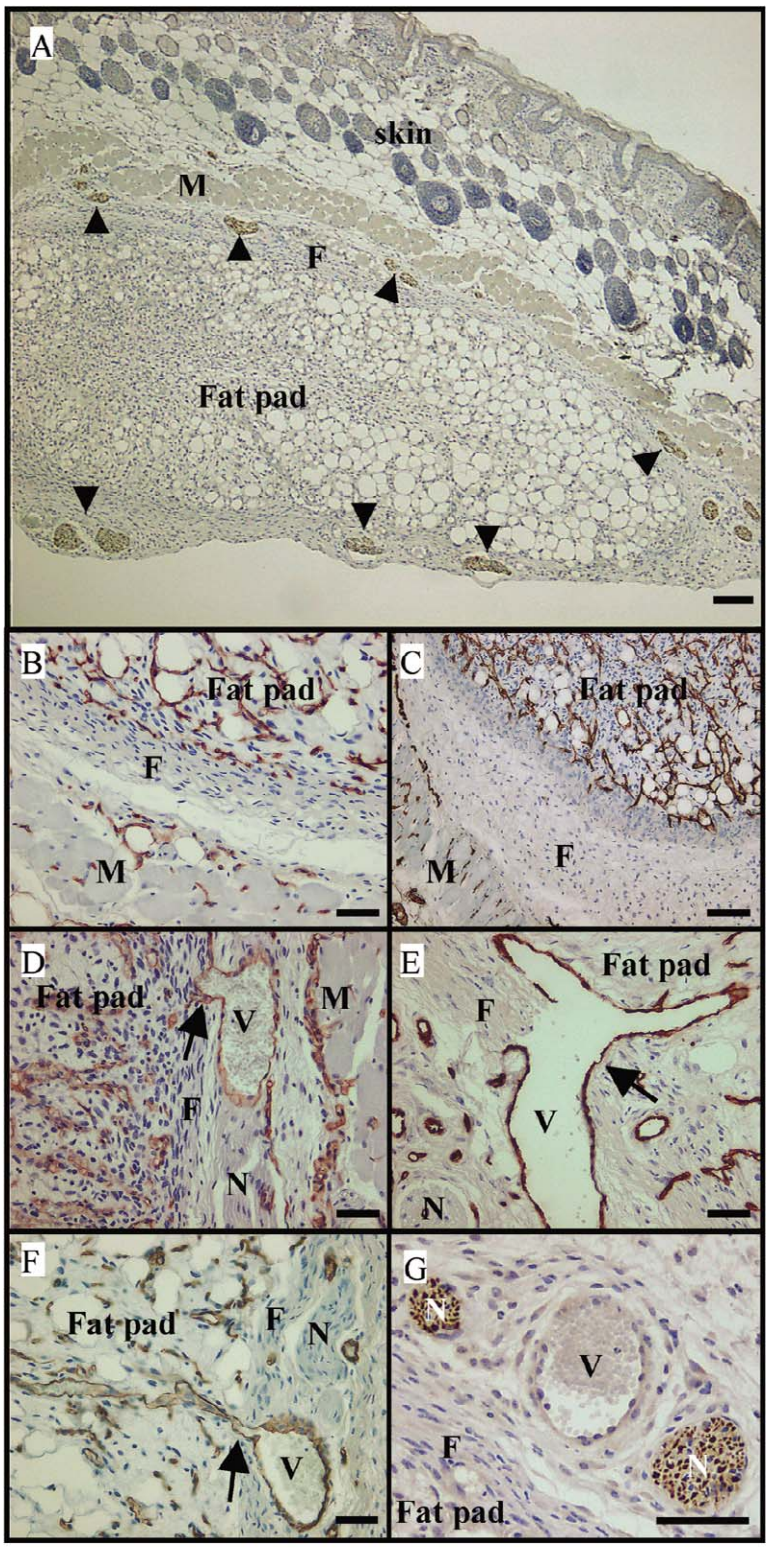

Figure 6. PECAM-1 and NF expression in the developing fat pads. (***A***) shows a relatively low power overview of a fat pad stained for neurofilament (brown), with the arrowheads indicating surrounding nerve bundles. (***B–F***) show immunohistochemical staining for PECAM-1 at the borders of different fat pads, illustrating the a-vascular fascia (***B***, ***C***) and blood vessels that sprout from nerve-associated blood vessels and protrude (arrows) through the fascia (***D–F***). (***G***) shows a higher magnification of a blood vessel associated with two nerve bundles and stained for neurofilament. *F*; fascia, *M*; muscle, *N*; nerve bundle, *V*; vessel. Scale bar = 100 μm in (***A***) and 50 μm in (***B–G***).